cussed above.

In the temperature range covered by the experiment the EFG increases slightly with decreasing temperature, in agreement with the behavior observed at higher temperatures by the angular correlation measurements. At $-196\,^{\circ}C$ the EFG acting on the Hf nuclei in $PbHfO_3$ is approximately 10% smaller than that acting on the Ta nuclei (see Table I). This difference is of the same size as found in HfO_2 and $(NH_4)_2HfF_6$.

ACKNOWLEDGMENTS

The authors are indebted to Professor E. Bodenstedt for his kind interest and support of this work. The generous support by the Bundesministerium für Bildung und Wissenschaft is gratefully acknowledged. The numerical calculations have been performed on the IBM 370 computer of the Rheinisch-Westfälisches Institute für Instrumentelle Mathematik.

*Fellow from Consejo Nacional de Investigaciones Cientificas y Tecnicas, Buenos Aires, Argentina.

[1]C. Kittel, Phys. Rev. 82, 729 (1951).

[2]E. Sawaguchi, A. Maniwa, and B. Hoshino, Phys. Rev. 83, 1078 (1951).

[3]A. P. Jain, S. N. Shringi, and L. M. Sharma, Phys. Rev. B 2, 2756 (1970).

[4]J. P. Canner, C. M. Yagvik, R. Gerson, and W. J. James, J. Appl. Phys. 42, 4708 (1971).

[5]G. Shirane, Phys. Rev. 86, 219 (1952).

[6]G. Shirane, E. Sawaguchi, and Y. Takagi, Phys. Rev. 84, 476 (1951).

[7]E. Sawaguchi, J. Phys. Soc. Japan 8, 615 (1953).

[8]F. Jona, G. Shirane, F. Mazzi, and R. Pepinsky, Phys. Rev. 105, 849 (1957).

[9]G. Shirane and R. Pepinsky, Phys. Rev. 91, 812 (1953).

[10]H. Frauenfelder and A. Steffen, in *Perturbed Angular Correlations*, edited by K. Karlsson, E. Matthias, and K. Siegbahn (North-Holland, Amsterdam, 1963).

[11]R. Béraud, I. Berkes, J. Danière, G. Marest, and R. Rouguy, Nucl. Instr. Methods 69, 41 (1969).

[12]K. Alder, E. Matthias, B. Olsen, and W. Schneider, in Ref. 10, p. 247.

[13]H. F. Wagner and M. Forker, Nucl. Instr. Methods 69, 197 (1969).

[14]M. Forker and J. D. Rogers, Nucl. Instr. Methods 96, 453 (1971).

[15]E. Gerdau, J. Wolf, H. Winkler, and J. Braunsfurth, Proc. Roy. Soc. (London) A311, 197 (1969).

[16]F. D. Feiock and W. R. Johnson, Phys. Rev. 187, 39 (1969).

[17]D. H. Anderson, J. Chem. Phys. 40, 1168 (1964).

[18]P. da R. Andrade, M. Forker, J. D. Rogers, and J. Kunzler, Phys. Rev. B 6, 2560 (1972).

[19]R. A. Cowley, Phys. Rev. 143, A981 (1964).

[20]V. G. Bhide and M. S. Multani, Phys. Rev. 139, 1983 (1965).

[21]W. Cochran, in *Advances in Physics*, edited by N. F. Mott (Taylor and Francis, London, 1960), Vol. 9, p. 387.

[22]Stelson and Grodzins, Nucl. Data Table A1, 21 (1965).

PHYSICAL REVIEW B VOLUME 7, NUMBER 3 1 FEBRUARY 1973

Compton Profile of Single-Crystal Vanadium

Walter C. Phillips*

Physics Department, Brandeis University, Waltham, Massachusetts 02154

(Received 26 June 1972)

The Compton profile of single-crystal vanadium has been measured with Mo $K\alpha$ x rays. The observed profile shows that the V band electrons are more spatially extended than the density calculated from Hartree–Fock V $3d$ functions. The measured anisotropy in the profile is significantly less than that calculated for free-atom $3d$ functions with an orbital population of 80% t_{2g}.

I. INTRODUCTION

The feasibility of using ~20 keV x rays for accurate single-crystal Compton investigations of $3d$ elements has recently been demonstrated for Fe by Phillips and Weiss.[1] We report here measurements in V using Mo $K\alpha$ (17.4 keV) x rays. The situation for V is experimentally somewhat more favorable than for Fe, because in V the ratio of elastic/Compton scattering is smaller and the $2s2p$ Compton threshold energies are lower.

We have measured the anisotropy in the Compton profile near $J(0)$ for the [110] zone, and the full profile for three crystal orientations. Our results are substantially in agreement with Compton measurements for polycrystalline V at 60 keV made using a Ge-Li detector and recently published by Paakari, Manninen, Inkinen, and Liukkonen.[2] The anisotropy we observe at $J(0)$ is smaller than predicted by earlier x-ray-diffraction measurements[3] of paired reflections in V, and corresponds to a nearly spherical $3d$ momentum (charge) density.

II. EXPERIMENT

The apparatus has been described previously.[1,4] The housing enclosing the V sample and Mo x-ray tube was evacuated in order to eliminate air scattering. A Soller collimator on the x-ray-tube window limited the angle between the extreme rays striking the sample to $\pm 3°$, and the mean Compton-scattering angle $2\theta_C = 157°$. The energy analysis of the scattered x rays was made with a LiF crystal using the (400) reflection and a pair of Soller collimators. The total instrumental resolution width (full width at half-maximum) was 0.31 a.u.

Two experimental procedures were followed: (i) the rotation experiment, in which a cylindrical V crystal was rotated about its axis, with the analyzer set at a fixed angle (wavelength) and (ii) the profile experiment, in which the V-crystal orientation was fixed and the analyzer swept through the wavelength range spanned by the Compton profile.

The rotation experiment measured anisotropy in the Compton profile in the [110] zone. The sample was a spark-machined oxygen-free V single-crystal cylinder with a [110] axis within 1° of the cylinder axis, which was oriented perpendicular to the scattering plane. To eliminate possible anisotropy due to sample or experimental geometry, the nominally $\frac{3}{8}$-in. cylinder diameter was spark machined to a tolerance of 0.001 in., and the cylinder positioned on the rotation axis with a runout of less than 0.002 in. In collecting the data the crystal was stepped at 3.6° ϕ angular intervals through many rotations. No anisotropy resulting from eccentricity (essentially having a 360° periodicity) was observed.

For the rotation experiment it was important to maintain a constant incident-beam intensity, since the low Compton-scattering intensity from V precluded using a monitor counter. The Norelco XRG5000 generator output had previously proved to be stable within $\pm 0.1\%$ over periods from minutes to days, but often the x-ray output of the spectrographic x-ray tubes had been found to be highly unstable. Investigation of several tubes showed that the instability was associated with focal-spot wandering and tube aging. For the rotation experiment a new tube was installed and the output stability carefully checked before, twice during, and after the experiment. All checks, for which a Be sample replaced the V crystal, showed the intensity of Compton scattering from the Be to be constant to within $\pm 0.2\%$ over times from 10 min to 2 days.

In the profile experiment measurements were made by scanning hundreds of times over the Compton line at 0.062-a.u. intervals. Data were obtained with the x-ray-scattering vector approximately along the [111], [221], and [241] crystal directions. The peak counting rate was 150 counts/min, and the $K\alpha$ Compton/background intensity was 4.5 at the peak. For each of the three crystal orientations, a total of ~30k x rays were counted per interval at the peak. The sample was an oxygen-free 0.21-in.-diam single-crystal cylinder with (110) faces cut perpendicular to the [110] cylinder axis. No impurity fluorescence was observed for this crystal. Several larger "pure" V single crystals were initially examined. All were found to contain trace Nb and/or Zr impurities, to which the analyzer is particularly sensitive because the Nb and Zr $K\alpha$ lines come in the wavelength region of the Mo $K\alpha$ Compton peak and are strongly excited by the incident Mo $K\alpha$ radiation. The magnitudes of the impurity lines were large enough to prevent the use of these crystals for the profile experiment. For the rotation experiment one of the larger crystals was used, since the small Nb $K\alpha$ impurity line came sufficiently far from the fixed wavelengths studied.

The three crystal orientations in the profile experiment were chosen in order to minimize Bragg scattering of the continuum radiation by the 16 sets of reflections which occur in the Compton wavelength region studied. In general, even with the crystal oriented to exclude most Bragg scattering, some elastic scattering will be present because of the broad temperature-diffuse-scattering (TDS) peaks. However, comparison of the data for the three profile experiments revealed no observable additional intensity in the vicinity of Bragg positions.

In the rotation experiment the [651] and [237] directions are close ($4.6 \pm 1°$) to the scattering plane, and the wavelength for Bragg scattering from these reflections is close (0.0023 and 0.0133 Å) to the two set analyzer wavelengths. Elastic scattering from these reflections (and probably also from the [008]) is present in the rotation data plotted in Fig. 1. However, the angular width $\Delta\phi$ over which elastic TDS scattering for each reflection occurs is ~7°, and thus the results provide Compton-anisotropy information over the remaining 70° of the [110] zone.

III. DATA ANALYSIS

The theory of Compton scattering on which the analysis is based is described in Refs. 5 and 6. When the electron binding energy E_B is small compared to the energy transferred to the electron in the collision (the impulse approximation), the Compton profile $J(z)$ and the one-electron ground-state momentum wave function $\chi_i(\vec{p})$ are related by the expression

$$J(z) = \tfrac{1}{2} \sum_i \int_{|z|}^{\infty} |\chi_i(\vec{p})|^2 \, dp_x \, dp_y \,, \tag{1}$$

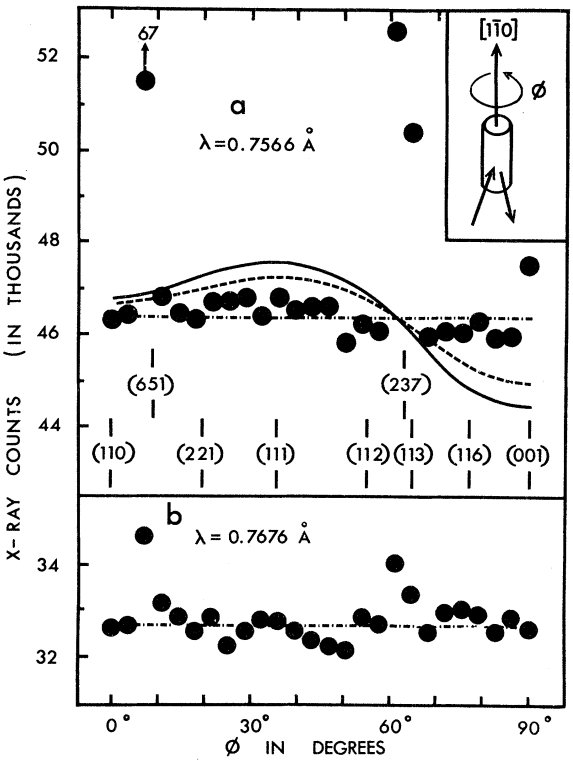

FIG. 1. Rotation experiment results at two wavelengths, folded into a 90° ϕ interval. The V crystal was rotated about a [110] axis, as shown in the inset. The angular positions of some crystal directions in the [110] zone are given. The size of the data points indicates the statistical uncertainty. The calculated curves are for the configurations (a) solid curve, and (b) dashed curve, discussed in the text, for an e_g/t_{2g} population ratio = 0.20/0.80.

where the scattering vector $\vec{k}-\vec{k}_0$ is perpendicular to the x-y plane,

$$\chi_i(\vec{p}) = (2\pi)^{-3/2}\int_0^\infty \psi_i(\vec{r})e^{-i\vec{p}\cdot\vec{r}}d^3r\ ,$$

$$z = \frac{mc}{2\lambda_0\sin\theta_C}\left(\Delta\lambda - \frac{2h}{mc}\sin^2\theta_C\right) \times\left[1+\Delta\lambda+\left(\frac{\Delta\lambda}{2\lambda_0\sin\theta_C}\right)^2\right]^{-1/2}, \quad (2)$$

λ_0 and λ are the wavelengths of the incident and scattered x rays, respectively, and $\Delta\lambda = \lambda - \lambda_0$. In order to obtain the experimental profile $J(z)$ the data (x-ray counts vs the LiF analyzer 2θ angle) were treated as follows. A smooth visual curve was drawn through the data. The background from Compton and TDS scattering of the bremsstrahlung continuum was approximated by a straight line. The slope and height of the background line were adjusted by trial and error until the resulting profile for $3.0 \le z \le 4.0$ a.u. agreed with that calculated for a Hartree–Fock (HF) V $2s^22p^63s^23p^63d^44s$ configuration,[7] and the difference between the background and the data below the $K\alpha$ threshold equaled the expected $K\beta$ Compton scattering. (The $K\beta$ Compton profile was estimated by scaling the measured $K\alpha$ profile.) With this background and the $K\beta$ background subtracted, the data were corrected for the wavelength dependence of the Compton cross section, the absorption in the sample, and the reflectivity of the LiF using the expression given by Eisenberger.[8] The $K\alpha_1$ and $K\alpha_2$ components of the Compton scattering were separated using the Rachinger method,[9] and the resulting profile was normalized so that

$$\int_0^{5.0} J(z)\,dz = 9.21 \text{ electrons},$$

the area calculated for the V HF $2s^22p^63s^23p^63d^44s$ configuration in the impulse approximation. It is not strictly correct to use the impulse approximation for the $2s^22p^6$ core. The energy transferred to the scattered electron at the Compton peak ($z=0$) is 1090 eV. The $3s$, $3p$, and $3d$ electrons satisfy the impulse-approximation condition, whereas the $2s$ and $2p$ electrons, $E_B = 628$ and 520 eV, do not. No available calculation treats scattering in the region where the energy transfer is of the order of E_B ($z \sim -2.5$ a.u.; see Fig. 2). Thus we are unable to knowledgeably calculate the area or subtract a calculated profile for the $2s^22p^6$ core in this region. Consequently, in the normalization and the final results reported below, $J(z)$ data for $z < 0.0$ (energy transfers $\lesssim 2E_B$) are not included. The experimental justification for using the impulse approximation for energy transfers $\gtrsim 2E_B$ ($z \gtrsim 0.0$) is discussed in Refs. 1 and 6.

IV. RESULTS AND DISCUSSION

A. Rotation Experiment

The rotation experiment measured anisotropy in the profile in the [110] zone. Small anisotropies can be studied relatively easily with this arrangement, whereas with the profile experiment the entire profile must be accurately measured before the data can be analyzed, and in the analysis itself background and $\alpha_1\alpha_2$ separation uncertainties can give rise to apparent anisotropies.

The measurements, shown in Fig. 1, were made at two analyzer wavelengths: $\lambda = 0.7566 \pm 0.0016$ Å ($z = 0.06$ a.u. for the α_1 contribution) and $\lambda = 0.7676 \pm 0.0016$ Å ($z = 1.11$ a.u. for the α_1 contribution). Except near the (651), (237), and (008) reflections for which the Bragg wavelengths are near the analyzer fixed wavelengths, the data near the α_1 peak [Fig. 1(a)] show only a small anisotropy, and the data off the α_1 peak [Fig. 1(b)] show essentially no anisotropy.

The two calculated curves shown in Fig. 1(a) are for the configurations which best fit the pro-

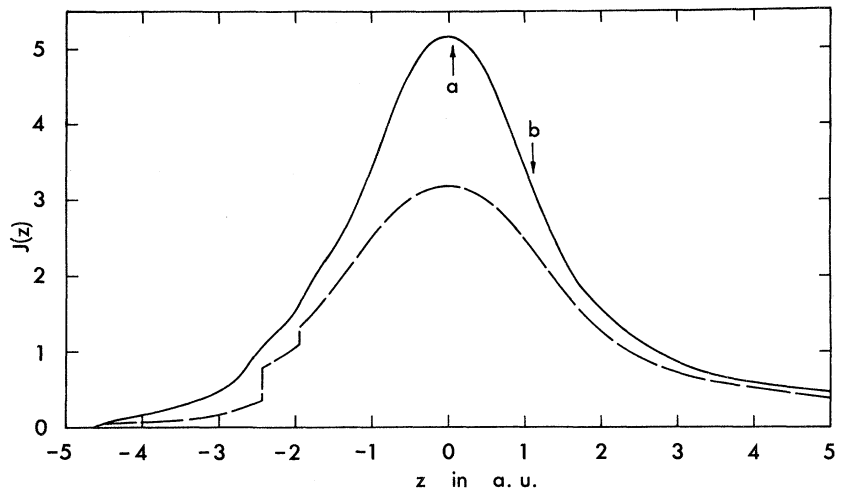

FIG. 2. Sum of the normalized V Compton profiles measured for the [111], [221], and [241] directions. Approximately 90k x rays were counted per 0.06-a.u. interval at the peak. The calculated impulse-approximation HF $2s^2 2p^6 3s^2 3p^6$ core profile is also plotted. The α_1 positions at which the rotation experiment measurements (Fig. 1) were made are indicated.

file-experiment results discussed below. For these the wave functions are (a) the HF V core $+5\{\text{Ti } 3d^4\}$, and (b) the HF V core $+4\{\text{V } 3d^5\}+1$ free electron, where $\{\text{Ti } 3d^4\}$ is a one-electron HF radial wave function calculated for a Ti $3d^4$ configuration. In order to calculate the anisotropy curves we used for the d electrons the doubly and triply degenerate $3d$ orbital description with an e_g/t_{2g} population ratio of 0.20/0.80. This population ratio was determined from x-ray-diffraction measurements of V paired reflections.[3] The Compton profile $J(z)$ per $3d$ electron is given by

$$J(z)=\frac{5}{2\pi}\int_{|z|}^{\infty}[j_2^*(pr)]^2\left[\alpha+\beta\left(\frac{z}{p}\right)^2+\delta\left(\frac{z}{p}\right)^4\right]_{t_{2g}}p\,dp\,,$$
$$j_2^*(pr)=\int_0^{\infty}Rj_2(pr)\,r^2\,dr\,, \tag{3}$$

with a corresponding expression for e_g, where R is the radial part of the $3d$ wave function and α, β, and δ are coefficients that depend on the relative orientation of the scattering vector and crystal axes.[10] The functions

$$\int_{|z|}^{\infty}[j_2^*(pr)]^2\left(\frac{z}{p}\right)^n p\,dp\quad(n=0,2,4) \tag{4}$$

have been evaluated by Weiss for the $3d$ functions given above.[11] The measurement includes contributions from both α_1 and α_2, and thus to calculate the total $3d$ Compton intensity [Fig. 1(a)] we assume that $\frac{2}{3}$ of the electrons are at $z=0.06$ a.u., corresponding to the α_1 contribution, and $\frac{1}{3}$ are at $z=-0.34$ a.u., corresponding to the α_2 contribution. To the d contribution must be added the rotation-independent contribution from the HF V core (calculated in Ref. 7), and for configuration (b) the free-electron contribution given by

$$J(z)=\frac{3}{4p_F}\left[1-\left(\frac{z}{p_F}\right)^2\right]\text{ per electron,} \tag{5}$$

where the Fermi momentum $p_F=0.68$ a.u. Finally, the rotation-independent background contribution $=1/4.5$ of the sum of the Compton contributions must be added. The rotation-independent contributions considerably reduce the magnitude of the observable Compton anisotropy. For example, for the 5 Ti $3d$ electrons the difference between the magnitude of the profile calculated for the [111] direction and the spherically averaged profile is 13%, i.e., $[J_{(111)}(0)-J_s(0)]/J_s(0)=0.13$, but when the α_2 and rotation-independent terms are added, the magnitude of the observable effect is only 2.7%.

Comparing the measurements and calculations in Fig. 1(a), it is clear that the anisotropy for either calculated configuration is greater than the anisotropy observed. Thus we conclude that the

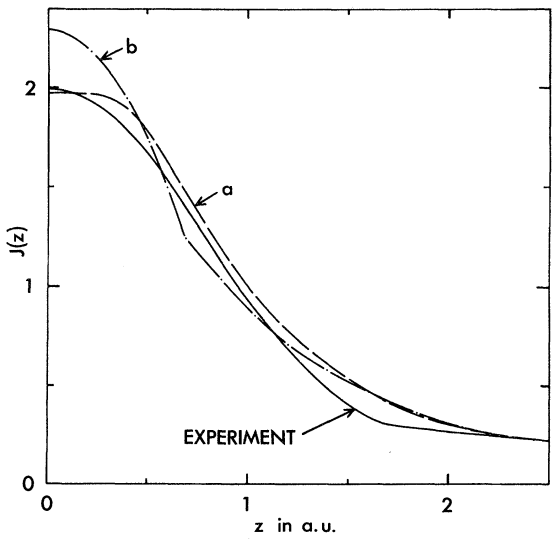

FIG. 3. Experimental band-electron profile (solid curve) and calculated profiles for (a) $5\{\text{Ti } 3d^4\}$, and (b) $4\{\text{V } 3d^5\}+1$ free electron, the models discussed in the text.

e_g/t_{2g} ratio is significantly closer to a 0.40/0.60 spherical configuration than the 0.20/0.80 ratio assumed for the calculation.

B. Profile Experiment

Within the experimental uncertainty no significant differences were observed between the profiles measured for the [111], [221], and [241] directions. The sum of these profiles, analyzed as described above, is shown in Fig. 2 and given in Table I. The uncertainty in $J(z)$ due to counting statistics is much smaller than the total experimental uncertainty, $\sim\pm 2\%$ at $J(0)$, due to background subtraction, $\alpha_1\alpha_2$ separation, and wavelength-dependent corrections.

The experimental band-electron profile, i.e., the difference between the average experimental $J(z)$ and the impulse-approximation core shown in Fig. 2, is plotted in Fig. 3 and given in Table I. Assuming the validity of the calculated core, the experimental uncertainty in the band-electron profile is ~5% at $J(0)$.

We have attempted to fit the band-electron profile using combinations of calculated $3d$ HF and free-electron profiles, and Eqs. (3) and (5). For the calculation we assumed a spherically symmetric $3d$ density, and to allow for correlation the free-electron profiles were scaled to the difference between the observed lithium band-electron profile[12] and the profile obtained from Eq. (5).

TABLE I. Measured and calculated V Compton profiles.

z	Measured $J(z)$	HF core $2s^22p^63s^23p^6$	Experimental band $J(z)$	(a) $5\{\text{Ti } 3d^4\}$	Calculated band profiles $4\{\text{V } 3d^5\}$ + F.E. = (b)		
0.0	5.16±0.10	3.17	1.99±0.10	1.97	1.34	0.95	2.29
0.1	5.14	3.16	1.98	1.97	1.34	0.93	2.27
0.2	5.09	3.14	1.95	1.97	1.34	0.86	2.20
0.3	4.98	3.11	1.87	1.95	1.33	0.76	2.09
0.4	4.84	3.06	1.78	1.89	1.31	0.63	1.94
0.5	4.67	3.00	1.67	1.77	1.26	0.48	1.74
0.6	4.44	2.91	1.53	1.62	1.19	0.29	1.48
0.7	4.19	2.82	1.37	1.45	1.10	0.13	1.23
0.8	3.93	2.71	1.22	1.29	1.01	0.10	1.11
0.9	3.67	2.59	1.08	1.13	0.92	0.08	1.00
1.0	3.40±0.07	2.47	0.93±0.07	1.00	0.83	0.06	0.89
1.1	3.14	2.34	0.80				
1.2	2.89	2.21	0.68				
1.3	2.66	2.08	0.58	0.69	0.61	0.03	0.64
1.4	2.44	1.95	0.49				
1.5	2.22	1.82	0.40				
1.6	2.02	1.69	0.33	0.48	0.45	0.02	0.47
1.7	1.87	1.58	0.29				
1.8	1.76	1.47	0.29				
1.9	1.65	1.37	0.28				
2.0	1.54±0.05	1.27	0.27±0.05	0.30	0.29	0.01	0.30
2.2	1.35	1.10	0.25				
2.4	1.19	0.98	0.21				
2.6	1.07	0.87	0.20				
2.8	0.96	0.79	0.17				
3.0	0.86±0.04	0.72	0.14±0.04	0.10	0.11		0.11
3.2	0.77	0.65	0.12				
3.4	0.71	0.61	0.10				
3.6	0.66	0.57	0.09				
3.8	0.62	0.54	0.08				
4.0	0.58±0.04	0.51	0.07±0.04	0.03	0.04		0.04
4.2	0.55	0.48	0.07				
4.4	0.53	0.45	0.08				
4.6	0.51	0.43	0.08				
4.8	0.49	0.41	0.07				
5.0	0.46±0.04	0.38	0.08±0.04	0.01	0.02		0.02

[This correlation correction reduces the calculated free-electron $J(0)$ by 15%.] The best fits were found for the HF profiles described above: (a) $5\{\text{Ti } 3d^4\}$ and (b) $4\{\text{V } 3d^5\}+1$ free electron. These profiles are shown in Fig. 3 and Table I. Since configuration (a) provides a reasonably good fit to the measured profile, we see, as expected, that in the solid the V band electrons are more spatially extended than in the free atom. The V profile recently calculated by Berggren[13] gives approximately equivalent agreement with the measured $J(z)$.

ACKNOWLEDGMENTS

We thank R. J. Weiss for much helpful advice and Professor C. G. Shull and P. L. Sagalyn for loaning the V crystals.

*Research supported by the National Science Foundation, Grant No. GU-3852.

[1]W. C. Phillips and R. J. Weiss, Phys. Rev. B (to be published).

[2]T. Paakori, S. Manninen, O. Inkinen, and E. Liukkonen, Phys. Rev. B 6, 351 (1972).

[3]R. J. Weiss and J. J. DeMarco, Phys. Rev. 140, A1223 (1965).

[4]W. C. Phillips and R. J. Weiss, Phys. Rev. 171, 790 (1968).

[5]P. Eisenberger and P. M. Platzman, Phys. Rev. A 2, 415 (1970).

[6]R. Currat, P. D. DeCicco, and R. J. Weiss, Phys. Rev. B 4, 4256 (1971).

[7]R. J. Weiss, A. Harvey, and W. C. Phillips, Phil. Mag. 17, 241 (1968).

[8]P. Eisenberger, Phys. Rev. A 5, 628 (1972).

[9]W. A. Rachinger, J. Sci. Instr. 25, 254 (1948).

[10]R. J. Weiss, Phil. Mag. 14, 403 (1966).

[11]R. J. Weiss, *X-Ray Determination of Electron Distributions* (North-Holland, Amsterdam, 1966), p. 185. These calculations employ $3d^n$ wave functions given by R. E. Watson, M.I.T. Solid State and Molecular Theory Group Tech. Rept. No. 12 (1959) (unpublished).

[12]W. C. Phillips and R. J. Weiss, Phys. Rev. B 5, 755 (1972).

[13]K. F. Berggren, Phys. Rev. B 6, 2156 (1972).

PHYSICAL REVIEW B VOLUME 7, NUMBER 3 1 FEBRUARY 1973

Fluctuations in $SrTiO_3$ near the 105-K Phase Transition

Th. von Waldkirch, K. A. Müller, and W. Berlinger
IBM Zurich Research Laboratory, CH-8803 Rüschlikon, Switzerland
(Received 24 July 1972)

The temperature dependence of the EPR linewidth of the Fe^{3+}-V_O pair center in $SrTiO_3$ has been investigated above and below $T_c = 105.6$ K. It is shown from the angular dependence that the pronounced line broadening near T_c results from rotational fluctuations of the oxygen octahedra. The analysis yields a changeover from a fast- to a slow-fluctuation regime for $T \to T_c^+$. The linewidth has a cusp-shaped behavior close to T_c and is finite at T_c. From measurements in samples transforming to monodomains below T_c the anisotropy of the fluctuations is investigated. It is found that they are anisotropic even for temperatures within 10 K *above* T_c, where the point symmetry of the crystal is cubic. In this region, the anisotropy is connected with the increasing regions of correlated motions. Well below T_c it is related to the two distinct soft-mode branches. The results are analyzed in terms of the dynamical form factor $S(\vec{q}, \omega)$. Within a certain approximation they are found to be consistent, for temperatures above and below T_c, with a value of the critical exponent ν (for the correlation length ξ) of $\nu \simeq 0.65$, together with a two-dimensionally anisotropic static-order-parameter susceptibility $\chi(\vec{q}, T)$ with an anisotropy parameter Δ of the order of $\frac{1}{40}$. The changeover from fast- to slow-fluctuation regime yields an estimate of the half-width of the central peak in $S(\vec{q}, \omega)$ of 70 MHz at $T = T_c + 0.8 \pm 0.3$ K.

I. INTRODUCTION

Strontium titanate undergoes a second-order antiferrodistortive phase transition from a cubic to a tetragonal low-temperature phase at $T_c \sim 105$ K, as has been known for a long time.[1-4] This transition is connected with a softening of the threefold-degenerate R_{25} phonon at the R corner ([111] zone boundary)[5,6] and consists of an alternate rotation of nearly rigid oxygen octahedra around one of the $\langle 100 \rangle$ axes. The staggered rotation angle φ is the generalized order parameter of the transition. Many of its static properties have been studied thoroughly,[4,7-10] and static critical phenomena have been observed near T_c in the temperature dependence of the order parameter.[11] In the present paper dynamical properties of the phase transition are investigated using electron paramagnetic resonance (EPR). Recently, it was found that the local rotational fluctuations of the octahedra near T_c can